"Modeling Plasma Processes in Gas Lasers"

R. F. Walter

Schafer Corporation
2309 Renard Pl. SE, Ste 300
Albuquerque, New Mexico 87106
USA

1. ABSTRACT

The repetitively-pulsed electron beam pumped excimer laser has been demonstrated to be capable of delivering high average power in the ultraviolet region of the spectrum. The results of recent experiments and comprehensive numerical modeling are presented. The experimental data were obtained from an electron beam pumped XeF laser with a decentered unstable resonator and a flowing gain medium. This device produced a pulse energy of 40 to 50 J at a pulse repetition frequency of 100 Hz. The numerical modeling was focused on providing detailed understanding of observed pulse shapes. These simulations involved two separate models: a detailed XeF kinetics code and an optical extraction code which is based on a novel stable resonator formulation. This integrated model was used to analyze and interpret the results of several recent experiments.

2. INTRODUCTION

The EMRLD Master Oscillator laser was developed by the AVCO Research Laboratory to operate with a pulse energy of 40 J at a wavelength of 353 nm and a pulse repetition frequency (PRF) of 100 Hz. 1 This XeF device is pumped by two opposing electron beam guns and provides a demonstration of the integration of e-beam systems with flow and acoustic technology with optical extraction techniques. The laser gas consists of a mixture of neon, xenon and nitrogen trifluoride (NF3) at a density of 3.9 amagats, which is circulated in a closed-cycle flow loop. The gas temperature can be varied between 300 K and 425 K. The present analyses address only experiments at room temperature. Excited xenon fluoride (XeF) is produced by direct e-beam pumping, and laser energy is extracted at 353 nm by a confocal unstable resonator. A schematic diagram of this resonator is presented in Figure 1. Note that windows separate the high pressure laser gas from the low pressure optical train. The magnification of the confocal unstable resonator is either 1.6 (at 300 K) or 2.5 (at elevated temperature). This resonator employs a decentered feedback mirror in order to produce a large unobscured output beam area.

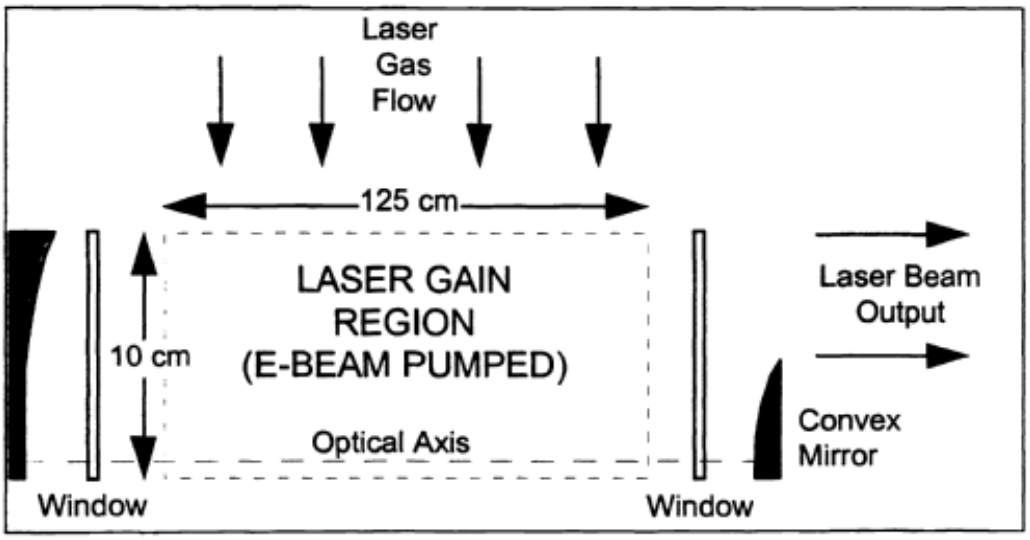

Figure 1. Laser resonator schematic.

Some aspects of the performance of the EMRLD laser were addressed previously in by Erkkila and Espander[2]. In particular, the effects of nonuniform pump power deposition on the spatial distribution of the output intensity were modeled with a Fox-Li unstable resonator model and a set of empirical expressions which related the gain, absorption, and saturation intensity of the laser medium to variations in the pump rate. In the present paper, the performance of this laser is analyzed using a novel optical extraction model based on a stable resonator formulation. This model is combined with a detailed XeF kinetics code which calculates the temporal variation of the gain, absorption, and saturation intensity for actual digitized pump power waveforms. The capability of the kinetics model to calculate these key parameters for arbitrary gas mixtures and conditions is a powerful feature of the present model. In the following sections, the basic elements of the overall model are described, and

some specific calculations are presented which help to elucidate some observed performance characteristics of the EMRLD laser device.

3. KINETICS MODEL

The XeF kinetics model which is employed in the present calculations has been described previously[3-4].
The model allows both Ne^+ and $Ne^•$ channels to contribute to the formation of the upper laser level. In each of these formation chains a Penning ionization process leads to the formation of Xe^+, which is the principal intermediary state from which the upper laser level is formed.

The present version of the XeF model consists of over 200 reactions involving more than 50 species. The computer code which is based on this model has been specially tailored to allow the user to test the effects of kinetic rate uncertainties on the laser performance predictions. The code employs a symbolic input/output format, and it provides a reaction monitor diagnostic which provides a tally of the most important reaction pathways. The code has an option to solve the Boltzmann equation to compute the energy distribution of the secondary electrons. In practice, it was found that this distribution function is sufficiently close to a Maxwellian distribution that it is acceptable to assume this functional form. Recently, the numerical integration routine has been improved to increase the robustness of the code and allow it to run over a wide range of input parameters.

4. OPTICAL EXTRACTION MODEL

The optical extraction analysis was based on a one dimensional, algebraic, temporal laser power extraction computer code. Known as PLASER, the gain cavity is divided into a series of thin gain sheets. Temporal small signal gain $(g_o)_{non}$-saturable absorption (α), and saturation intensity (I_{sat}) are inputs to the code. Arrays which represent these quantities are configured with sets of values corresponding to each resonator round trip. PLASER models the laser as a Fabry-Perot (stable) resonator with no diffraction losses. Resonator parameters consist of mirror reflectivities, window transmission losses, mirror spacing and output area. All cavity fluxes are initially set to zero. A noise flux starts out from the outcoupler end of the laser [$I_f(1)$] and enters the first gain sheet. This intensity is modified as it passes through each gain sheet according to the following equation:

$$I_f(n+1) = I_f(n) \times e^{\left[\frac{g_o(r)}{1 + \frac{I_f(n)+I_b(n)}{I_{sat}(r)}} - \alpha(r)\right] dz}$$

Here dz is the thickness of the gain sheet. When the flux reaches the end of the gain length it is multiplied by the window transmission and rear mirror reflectivity to create the backward wave [$lb(n_{total})$].

$$I_b(n_{total}) = I_f(n_{total}+1) \times t_{window} \times r_{mirror} \times t_{window}$$

The backward wave is propagated through the gain according to the following equation:

$$I_b(n-1) = I_b(n) \times e^{\left[\frac{g_o(r)}{1 + \frac{I_f(n)+I_b(n)}{I_{sat}(r)}} - \alpha(r)\right] dz}$$

At the end of the gain length the intensity is multiplied by the window losses and mirror reflectivity. The output and feedback intensities are calculated and the gain, absorption, and saturation intensities are updated.

$$I_f(1) = I_b(0) \times t_{window} \times r_{outcoupler} \times t_{window}$$

$$I_{out}(t) = [I - I_f(1)] \times I_{sat}$$

Since the saturation intensity is changing, the feedback intensity must be re-nonnalized to the new saturation intensity.

$$I_f'(1) = I_f(1) \times \left(\frac{I_{sat}}{I_{sat}'}\right)$$

The process is repeated until the laser turns off. The temporal output intensities are multiplied by the output area and integrated to calculate the total output energy.

5. LASER PERFORMANCE

For the present analyses, we assumed that energy was deposited uniformly throughout the gain volume at each instant of time; this pump rate is given by the sum of the product of voltage and current from the two e-guns (referred to as the North and South e-guns because of their position in the laboratory). The temporal history of this deposited pump power is plotted in Figure 2. Note that the average pump power during the 1.25-microsecond pulse is 134 kW/cm^3. The total deposited pump energy is 206.4 J/liter.

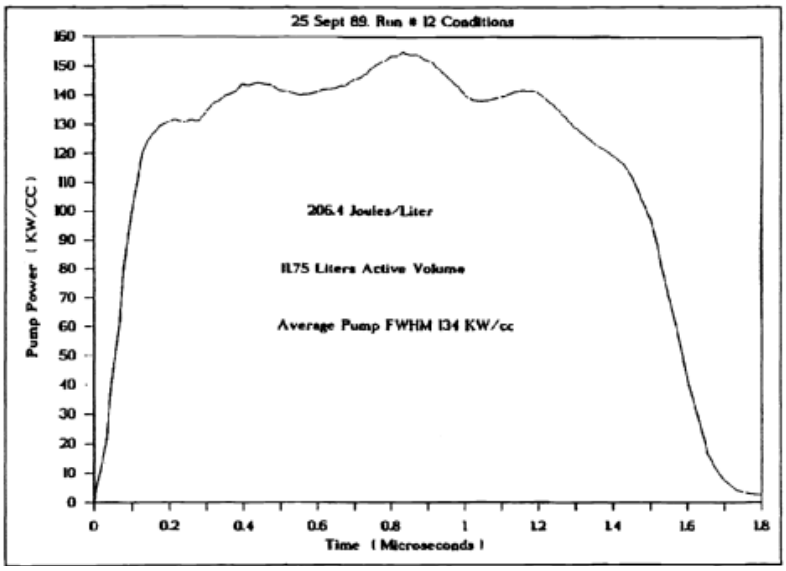

Figure 2. Temporal history of deposited pump power.

The pump temporal history was used as input to the XeF kinetics code, which was used to calculate the time variation of the small-signal gain and nonsaturable absorption during the pulse. The quantities are plotted in Figure 3. The calculated gain and absorption values, together with the saturation intensity, were then used as inputs to the PLASER model, which computed the laser output intensity as a function of time. The PLASER model calculated a total output energy of 46.2 J for this run, which is in very good agreement with the measured value of 46.0 J. The temporal history of the output intensity clearly followed that of the pump pulse and the gain.

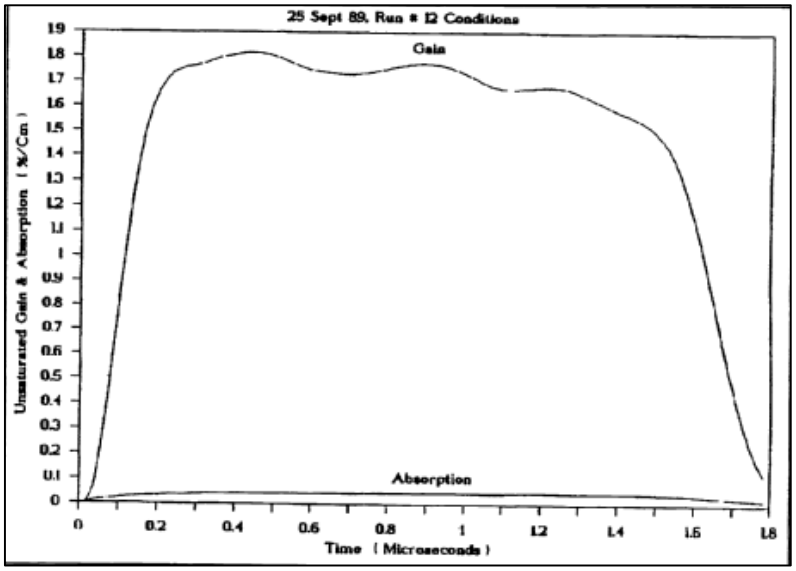

Figure 3. EMRLD MO gain and absorption vs. time

However, the measured time variation of the laser output intensity (Figure 4) exhibits a more rapid decay on the trailing edge of the pulse than does the PLASER prediction based on kinetics code outputs. We attempted to identify the cause of this discrepancy by examining the behavior of the sidelight fluorescence from the EMRLD device, which was measured separately

with no laser extraction (Figure 5). Note that the fluorescence, which is proportional to the XeF upper laser level number density, also exhibits this rapid decay after 0.4 microseconds. If the small signal gain is assumed to follow this temporal variation, with an average value corresponding to that measured in separate experiments,[5] the PLASER model can be made to calculate a time history of the output intensity which is very similar to the measured time variation. In this case the predicted output energy is 45.1 J, which is still in close agreement with the measured value of 46.0 J.

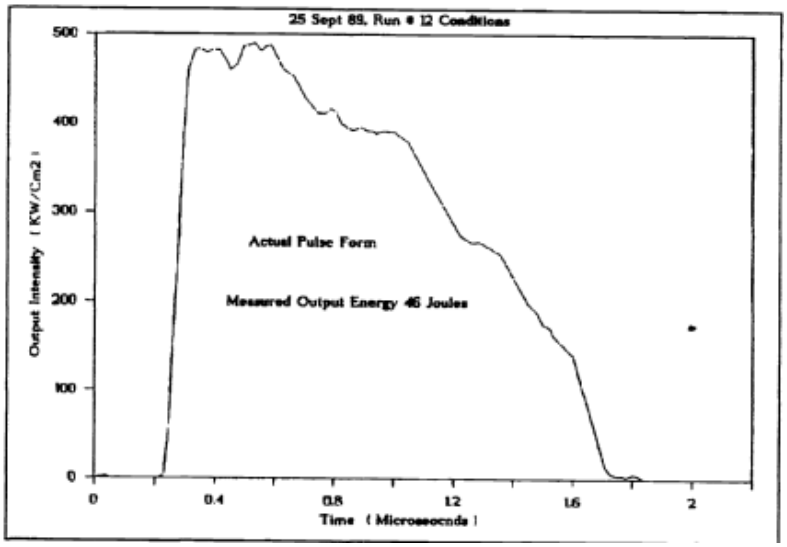

Figure 4. EMRLD MO Output intensity vs. time

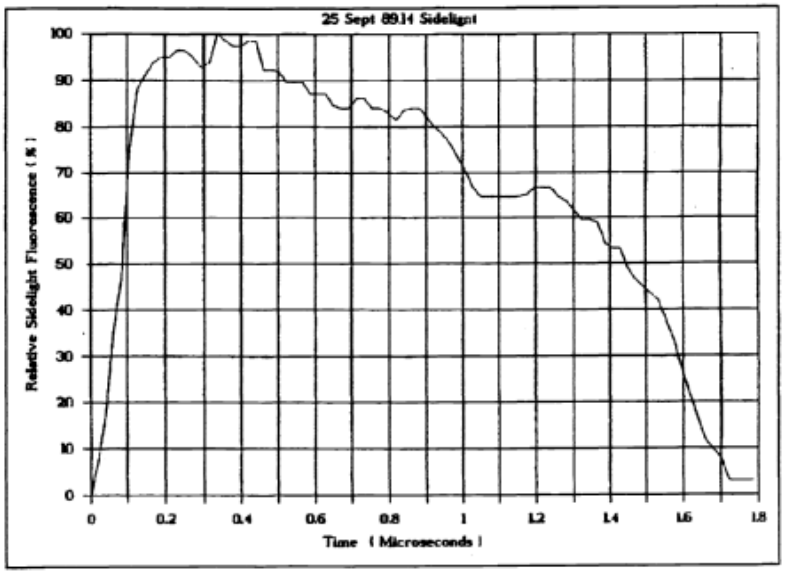

Figure 5. Relative Sidelight fluorescence vs. time.

We believe that the principal reason for the discrepancy in the detailed temporal pulse shapes lies in the fact that the XeF kinetics model does not contain any temperature-dependent kinetic rates at the present time. Moratz, et al. have reported that the gas temperature rise late in the pulse can have an important effect on kinetic performance, especially for lasers with energy loadings in excess of 200 J/liter.[6] Since our XeF kinetics model has been anchored primarily to pulse-averaged data, it is perhaps not surprising that its constant-temperature rate pack- age provides good agreement with pulse energy but not detailed pulse shape. We are currently adding temperature- dependent kinetic rates to this model to test this hypothesis.

6. PARAMETER STUDIES

In addition to performing calculations for the set of device parameters appropriate to the design point and the exact run conditions of specific tests, we varied a number of parameters to assess the potential for increasing the laser output energy. These calculations were undertaken because it was recognized that some parameter values, in particular the window transmission, can change with time. In these circumstances, the selection of an optimum out- put coupling based on an assumed set of window losses can lead to laser performance

which is far from optimal after the loss has increased as a result of chemical contamination. The output coupling of 61% associated with the M = 1.6 unstable resonator yields an output energy of 46.1 J, compared to a maximum of 48.8 J which could be obtained at a lower output coupling of 45%. This difference reflects the uncertainty in kinetic performance at the time the laser design point was selected.

After the experiments with the M = 1.6 unstable resonator were completed, a stable resonator with a 50% output coupling was installed on the EMRLD laser. The PLASER model predicted an output energy of about 47 J for the same gas mix, pump rate, and window loss values which were used in the unstable resonator experiments. However, the output energy with the stable resonator was only 37.7 J. The PLASER model was used to assess the causes of this discrepancy. After varying a number of parameters over the range of uncertainty associated with them, we concluded that the most likely cause of the low output energy was a degradation in the window loss from 0.5%/window to about 3.5%/window. Such a loss is considered within the range of possible values and may have resulted from the accumulation of contaminant species on the window surface during the resonator configuration change.

7. SUMMARY

A multi-stage model was developed to calculate the performance of pulsed XeF lasers. The model em- ploys a detailed kinetics code to calculate the gain, absorption, and saturation intensity parameters for arbitrary gas mixtures and pump pulse waveforms. These calculated quantities are used with an extraction model based on a stable resonator formulation. It was found that this simple model gave excellent agreement with experimental results for unstable as well as stable resonators. Hence, it is unnecessary to employ more sophisticated unstable resonator extraction models if pulse energy alone is the desired output characteristic from the calculation.

8. REFERENCES

1. Smiley, V. N., SPIE Technical Symposium on Lasers and Optical Computing, Paper No. 1225-01, Los Angeles, California, 1990.

2. Erkkila, J. H. and Espander, W. R., SPIE Technical Symposium on Lasers and Optical Computing, Paper No. 1224-42, Los Angeles, California, 1990.

3. Finn, T. G., Palumbo, L. J. and Champagne, L. F., "A Kinetics Scheme for the XeF Laser," Appl. Phys. Lett., 33, 148, 15 July 1978.

4. Johnson, T. H., Palumbo, L. J. and Hunter, III, A.M., "Kinetics Simulation of High-Power Gas Lasers," IEEE J. Quant. Elec., QE-15, 289, May 1979.

5. Mandl, A. E. and Hyman, H. A., "XeF Laser Performance for F_2 and NF_3 Fuels," IEEE J. Quant Elec., QE-22, 349, February 1986.

6. Moratz, T. J., Saunders, T. D. and Kushner, M. J., "High-Temperature Kinetics in He and Ne buffered XeF Lasers: The Effect on Absorption," Appl. Phys. Lett., 54, 102, 9 January 1989.